NREL
NATIONAL RENEWABLE ENERGY LABORATORY

Influence of Atmospheric Variations on Photovoltaic Performance and Modeling Their Effects for Days with Clear Skies

Preprint

Bill Marion

Presented at the 2012 IEEE Photovoltaic Specialists Conference
Austin, Texas
June 3–8, 2012

NREL is a national laboratory of the U.S. Department of Energy, Office of Energy Efficiency & Renewable Energy, operated by the Alliance for Sustainable Energy, LLC.

Conference Paper
NREL/CP-5200-54130
June 2012

Contract No. DE-AC36-08GO28308

NOTICE

Available electronically at http://www.osti.gov/bridge

Available for a processing fee to U.S. Department of Energy
and its contractors, in paper, from:

U.S. Department of Energy
Office of Scientific and Technical Information

P.O. Box 62
Oak Ridge, TN 37831-0062
phone: 865.576.8401
fax: 865.576.5728
email: mailto:reports@adonis.osti.gov

Available for sale to the public, in paper, from:

U.S. Department of Commerce
National Technical Information Service
5285 Port Royal Road
Springfield, VA 22161
phone: 800.553.6847
fax: 703.605.6900
email: orders@ntis.fedworld.gov
online ordering: http://www.ntis.gov/help/ordermethods.aspx

Cover Photos: (left to right) PIX 16416, PIX 17423, PIX 16560, PIX 17613, PIX 17436, PIX 17721

Printed on paper containing at least 50% wastepaper, including 10% post consumer waste.

Influence of Atmospheric Variations on Photovoltaic Performance and Modeling Their Effects for Days with Clear Skies

Bill Marion
National Renewable Energy Laboratory, 15013 Denver West Parkway, Golden, CO 80401

ABSTRACT

Although variation in photovoltaic (PV) performance is predominantly influenced by clouds, performance variations also exist for days with clear skies with different amounts of atmospheric constituents that absorb and reflect different amounts of radiation as it passes through the Earth's atmosphere. The extent of the attenuation is determined by the mass of air and the amounts of water vapor, aerosols, and ozone that constitute the atmosphere for a particular day and location.

Because these constituents selectively absorb radiation of particular wavelengths, their impact on PV performance is sensitive to the spectral response of the PV device. The impact may be assessed by calculating the spectral mismatch correction. This approach was validated using PV module performance data at the National Renewable Energy Laboratory for summer, fall, and winter days with clear skies. The standard deviations of daily efficiencies for single-crystal Si, a-Si/a-Si/a-Si:Ge, CdTe, and CIGS PV modules were reduced to 0.4% to 1.0% (relative) by correcting for spectral mismatch, temperature, and angle-of-incidence effects.

INTRODUCTION

The ability to accurately determine the performance of a photovoltaic (PV) system is important for meeting contractual obligations of buyers and sellers, and for determining changes in performance that have occurred over time. Additionally, the same techniques may be incorporated into improved PV performance models for more accurate predictions of energy yield.

Clouds primarily influence the performance variability of PV systems, but variations also exist for days with clear skies with different amounts of atmospheric constituents that absorb and reflect different amounts of radiation as it passes through the Earth's atmosphere. The extent of the attenuation is determined by the mass of air and the amounts of water vapor, aerosols, and ozone that constitute the atmosphere for a particular day and location.

Because these constituents selectively absorb radiation of particular wavelengths, their impact on PV performance is sensitive to the spectral response of the PV device. Although the impacts are generally small, they may exhibit seasonal or geographic trends that increase variability in PV performance measurements from season to season, by location, or, in some instances, from day to day.

The impact of variations in atmosphere was assessed by calculating the spectral mismatch correction for summer, fall, and winter days with clear skies at the National Renewable Energy Laboratory (NREL) and applying the spectral mismatch correction, along with corrections for angle-of-incidence effects and PV module temperature, to the measured daily efficiencies of single-crystal Si, a-Si/a-Si/a-Si:Ge, CdTe, and CIGS PV modules. Daily efficiencies were judged a more suitable metric than peak power because: 1) they are more indicative of the energy produced over a range of irradiances; 2) summing the measured irradiances for a daily total reduces the uncertainty of the irradiance; and 3), some of the spectral model inputs, such as aerosol optical depth, precipitable water vapor, and ozone, are more readily available as daily values.

SPECTRAL MISMATCH CORRECTION

The approach for accounting for spectral variations was to model the solar spectrum, and to use it with the PV module's spectral response to calculate and apply a spectral mismatch correction, similar to principles developed by Osterwald [1] for translating device performance to reference conditions.

The Simple Model of the Atmospheric Radiative Transfer of Sunshine Version 2 (SMARTS) [2] was used to model spectral irradiance for calculating the spectral mismatch correction. Developed by Gueymard, SMARTS provides direct normal, global and diffuse horizontal, and global tilted spectral irradiances for clear skies and for 2,002 wavelengths from 280 to 4,000 nm [3]. It has been shown to be as accurate as more complex models such as the U.S. Air Force's MODTRAN [4]. This work uses SMARTS Version 2.9.5. An earlier Version 2.9.2 was used to develop the G173-03 reference solar spectral irradiances [5].

The general form of the spectral mismatch correction M is represented by Eqn. 1. A value of M = 1.0 indicates that there is no spectral mismatch with regard to the reference spectrum. A value greater than one indicates that the spectral distribution of the incident radiation for the device being tested is more favorable than if the incident radiation were the reference spectral condition; consequently, the PV performance is increased proportionally (the converse applies for values less than one).

$$M = \frac{\int_a^b E_{ref}(\lambda)\cdot S_r(\lambda)d\lambda}{\int_a^b E_{inc}(\lambda)\cdot S_r(\lambda)d\lambda} \cdot \frac{\int_c^d E_{inc}(\lambda)\cdot S_t(\lambda)d\lambda}{\int_c^d E_{ref}(\lambda)\cdot S_t(\lambda)d\lambda} \quad (1)$$

where:

λ = wavelength
a,b = integration limits, should include response range of reference device
c,d = integration limits, should include response range of device being tested
$E_{ref}(\lambda)$ = spectral irradiance for reference condition
$E_{inc}(\lambda)$ = spectral irradiance incident on device being tested
$S_r(\lambda)$ = spectral response of reference device
$S_t(\lambda)$ = spectral response of device being tested.

Derived from Eqn. 1, Eqn. 2 is the specific form of the spectral mismatch correction for this work that models the spectral solar irradiance with SMARTS and measures the broadband solar irradiance with a Kipp & Zonen CM11 pyranometer as the reference device. The numerator of the first term, 992.43 W/m^2, is the integrated solar irradiance of the G 173-03 reference spectrum from 310 to 2,800 nm, which includes the complete spectral range of the Kipp & Zonen pyranometer. The spectral response of the Kipp & Zonen pyranometer is assumed constant over its spectral range.

$$M = \frac{992.43 W/m^2}{\int_{310}^{2800} E_{SMARTS}(\lambda)d\lambda} \cdot \frac{\int_{280}^{4000} E_{SMARTS}(\lambda)\cdot S_t(\lambda)d\lambda}{\int_{280}^{4000} E_{G173}(\lambda)\cdot S_t(\lambda)d\lambda} \quad (2)$$

where:

$E_{SMARTS}(\lambda)$ = SMARTS spectral irradiance, W m^{-2} nm^{-1}.
$E_{G173}(\lambda)$ = G173-03 reference hemispherical solar spectral irradiance, W m^{-2} nm^{-1}.

For applying a spectral correction to the daily summation of the plane-of-array irradiance, Eqn. 3 provides an expression for the daily spectral mismatch correction M_d.

$$M_d = \frac{\sum_{i=1}^{i=n} M_i \cdot E_i}{\sum_{i=1}^{i=n} E_i} \quad (3)$$

where:

E = irradiance, W m^{-2}
n = number of data values for the day.

CLEAR-SKY DAYS AT NREL

To represent days with clear skies and for a range of solar geometries encompassing seasonal variations for NREL's location, we selected summer, fall, and winter days for analysis. The longitude and latitude for NREL is W105.18° and N39.74°, and the elevation is1,829 meters. Days were selected by examining daily profiles of direct normal and plane-of-array solar radiation and choosing days exhibiting smooth sinusoidal-shaped solar radiation profiles without vertical perturbations indicating the presence of clouds.

Because of the local climate and weather, more clear days were present in September than in the other months evaluated (June, July, December, and January). Although December was evaluated, no clear-sky days were present; consequently, winter solar geometry and conditions are represented by the two clear-sky days in January.

The selected clear-sky days at NREL are listed in Table 1, which also includes the average meteorological conditions for each day used for input parameters for the SMARTS model. Atmospheric pressure (p) was measured at NREL; precipitable water vapor (w) and aerosol optical depth at 500 nm (τ_{a5}) data are from the AERONET station in nearby Boulder, CO [6]; and ozone (O_3) data are from NASA's total ozone mapping project [7].

Table 1. Clear-Sky Days and Meteorological Conditions

Day	p (mbar)	w (cm)	τ_{a5}	O_3 (atm-cm)
6/15/10	817.8	0.854	0.069	0.312
6/17/10	813.9	0.645	0.063	0.316
6/28/10	820.3	1.380	0.091	0.311
6/30/10	820.2	1.143	0.083	0.310
7/05/10	816.5	1.662	0.103	0.257
9/03/10	825.4	0.795	0.063	0.289
9/06/10	814.7	0.295	0.060	0.303
9/11/10	821.6	0.493	0.045	0.290
9/17/10	819.7	0.930	0.089	0.278
9/19/10	818.3	0.730	0.057	0.264
9/25/10	826.9	1.032	0.058	0.264
9/26/10	822.4	0.950	0.044	0.265
9/28/10	820.0	0.907	0.052	0.254
9/29/10	820.6	1.259	0.095	0.256
9/30/10	822.3	1.163	0.086	0.266
1/07/11	814.9	0.728	0.030	0.269
1/21/11	815.4	0.330	0.019	0.278

Table 2. Sensitivity of Daily Spectral Mismatch Correction to Day of Year and Meteorological Conditions

Model Inputs	Reference	Singular Change in Model Input Values									
Date	9/22/10	6/21/10	12/21/10	–	–	–	–	–	–	–	–
p (mbar)	821.2	–	–	813.9	826.9	–	–	–	–	–	–
w (cm)	0.855	–	–	–	–	0.295	1.662	–	–	–	–
τ_{a5}	0.065	–	–	–	–	–	–	0.019	0.103	–	–
O_3 (atm-cm)	0.273	–	–	–	–	–	–	–	–	0.254	0.316
Results		Change Relative to Results in the Reference Column (%)									
DNI (kWh/m^2/day)	9.85	25.8	-32.6	0.1	-0.1	5.0	-3.7	7.1	-5.2	0.1	-0.3
E (kWh/m^2/day)	7.81	-1.1	-27.7	0.1	-0.1	4.2	-3.2	1.4	-1.0	0.1	-0.2
M_d Single-Crystal Si	0.986	-2.0	3.1	0.0	0.0	-0.9	0.4	-0.5	0.1	0.0	0.0
M_d a-Si/a-Si/a-Si:Ge	1.022	-0.1	-10.8	0.0	0.0	-3.5	2.5	0.3	0.0	0.1	-0.3
M_d CdTe	0.993	0.6	-1.6	0.0	0.0	-3.0	2.1	0.1	0.0	0.0	-0.1
M_d CIGS	0.991	-1.2	1.7	-0.1	0.0	-1.0	0.4	-0.3	0.0	0.0	0.0

-- Denotes same value as the value in the reference column.

SPECTRAL MISMATCH SENSITIVITY

An analysis was performed to examine the sensitivity of the daily spectral mismatch correction of the four PV technologies (single-crystal Si, a-Si/a-Si/a-Si:Ge, CdTe, and CIGS) to changes in season and for the variations in meteorological conditions of Table 1. As a reference, daily spectral mismatch corrections were calculated usingSMARTS modeled spectra for the fall equinox (September 22, 2010) for PV modules oriented south and tilted from the horizontal at an angle equal to the latitude. Spectra were modeled for every 5 minutes of the day. Meteorological inputs to SMARTS were the September averages of the meteorological data from Table 1.

The reference results are shown as the second column in Table 2. For the single-crystalline silicon, CdTe, and CIGS PV modules, the daily spectral mismatch correction values indicate that PV performance is about 1% less than if the spectral irradiance distribution matched the G173-03 reference spectrum. For the a-Si/a-Si/a-Si:Ge PV module, PV performance is increased about 2%. The remaining columns show the percentage change in solar radiation and daily spectral mismatch corrections as model inputs are singularly changed from the values in the second column. The model input values were changed to include the summer and winter solstice, and the minimums and maximums of the meteorological data from Table 1.

For the summer solstice (June 21) model runs, the other meteorological inputs were left unchanged to show the effects of the reduced path length through the atmosphere or air mass. This shows a slight benefit for the CdTe PV module, with its daily spectral mismatch correction increased by 0.6%. The other module mismatch corrections are reduced, up to 2% for the crystalline silicon PV module.

For the winter solstice (December 21) model runs, the air mass is increased. This is beneficial for the CIGS PV module (+1.7%) and the crystalline silicon PV module (+3.1%), whereas the daily spectral mismatch correction is decreased for the CdTe PV module (-1.6%) and the a-Si/a-Si/a-Si:Ge PV module (-10.8%).

Varying the meteorological conditions to reflect the minimums and maximums from Table 1 yielded essentially no change in daily spectral mismatch corrections over the range of pressures encountered, and only slight changes when changing ozone amounts (-0.3% for the a-Si/a-Si/a-Si:Ge PV module). Varying aerosol amounts yielded somewhat greater change in daily spectral mismatch corrections (-0.5% to 0.3%). Largest changes in spectral mismatch corrections resulted from changing precipitable water vapor. The minimum precipitable water vapor value decreased the spectral mismatch correction (-0.9% to -3.5%) and the maximum precipitable water vapor value increased the spectral mismatch correction (+0.4% to +2.5%). The CdTe and a-Si/a-Si/a-Si:Ge PV modules are more sensitive to changes in precipitable water vapor than the other PV modules.

Although Table 2 treats parameters that influence spectral irradiance independently, in nature, parameters may exhibit dependency. For example, in winter, the amounts of aerosol and water vapor are decreased. Consequently, we can expect in practice that the crystalline silicon and CIGS PV modules will have a somewhat less beneficial spectral correction in winter than shown in the Table 2 because the advantage of increased air mass is offset somewhat by the disadvantage of lower aerosol and water vapor amounts.

VALIDATION WITH PV PERFORMANCE DATA

The method of using a daily spectral mismatch correction to account for variations in meteorological conditions was validated using PV module performance data at NREL for the summer, fall, and winter days with clear skies. The validation metric was the standard deviation of daily efficiencies for single-crystal Si, a-Si/a-Si/a-Si:Ge, CdTe, and CIGS PV modules after correcting for spectral mismatch, temperature, and angle-of-incidence effects.

PV Performance Data

NREL's Performance and Energy Rating Test bed (PERT) provided the PV performance data. The data include current-voltage (I-V) curves measured at 15-min intervals with coincident measurements of POA irradiance and PV

module back-surface temperatures. PV cell temperatures were estimated by adding 3.0°C per 1000 W/m^2 irradiance to the PV module back-surface temperature [8].

Daily Efficiency

For each of the days with clear skies, the daily efficiency, η, was calculated for each PV module using Eqn. 4.

$$\eta = \frac{\sum_{i=1}^{i=n} P_i}{A \cdot \sum_{i=1}^{i=n} E_i} \quad (4)$$

where:

P = PV module power, W
A = PV module area, m^2

Temperature Correction

The Standard Reporting Condition (SRC) temperature is a PV module cell temperature of 25°C. This temperature is recognized as not being representative of the operating temperatures of most PV systems. A temperature more representative of actual field operation is the irradiance-weighted cell temperature, T_{iw}, defined by Eqn. 5.

$$T_{iw} = \frac{\sum_{i=1}^{i=n} T \cdot E_i}{\sum_{i=1}^{i=n} E_i} \quad (5)$$

where:

T = PV module cell temperature, °C.

Using data for all the days with clear skies in September, Eqn. 5 was used to calculate an irradiance-weighted Reporting Condition (RC) temperature, T_{rc}, for each PV module.

Temperature coefficients, when expressed in units of per °C, are normalized by the parameter value at the rating condition. If the reporting condition temperature is changed, the temperature coefficient is also changed because the parameter value at the new reporting condition changes. Equation 6 provides the relationship between the temperature coefficient of power at reporting conditions (γ_{rc}) and that at SRC (γ_0). Zero subscripts denote SRC.

$$\gamma_{rc} = \frac{\gamma_0}{\left[1 + \gamma_0 \cdot \left(T_{rc} - T_0\right)\right]} \quad (6)$$

Table 3 provides the irradiance-weighted RC temperatures for each PV module, and their temperature coefficient of power at both the SRC and RC.

Table 3. PV Module Reporting Condition Temperatures and Coefficients of Power at SRC and RC

PV Module	T_{rc} (°C)	γ_0 (°C^{-1})	γ_{rc} (°C^{-1})
Single-crystal Si 0442	51.7	-0.0045	-0.0051
a-Si/a-Si/a-Si:Ge 1736	47.9	-0.0024	-0.0026
CdTe 5669	54.6	-0.0025	-0.0027
CIGS 5165	48.9	-0.0042	-0.0047

Equation 7 adjusts the daily efficiency from Eqn. 4 to a temperature-corrected value, η_T, corresponding to the RC temperature.

$$\eta_T = \frac{\eta}{\left[1 + \gamma_{rc} \cdot \left(T_{iw} - T_{rc}\right)\right]} \quad (7)$$

where:

T_{iw} = Irradiance-weighted temperature for the day, from Eqn. 5, °C.

Angle-of-Incidence Correction

The angle-of-incidence (AOI) correction accounts for increased reflection losses when the incident angle of the solar radiation impinging the module surface increases. A correction by Sjerps-Koomen et al. [9] based on Fresnel equations for an air/glass interface was used to calculate a derate factor, F_{AOI}, which provides the useable fraction of the daily POA irradiance not lost to AOI effects.

$$F_{AOI} = 1 - \frac{\sum_{i=1}^{i=n} L_i}{\sum_{i=1}^{i=n} E_i} \quad (8)$$

where:

L = irradiance lost to AOI effects, W m^{-2}

For the PV modules with fixed latitude-tilt orientation, AOI losses are greater in summer (3%) than winter (1%) because AOI values are greater. Days with clear skies in September were used to calculate an AOI derate factor for RC, F_{AOIrc}. Values of F_{AOIrc} are 0.981 for the PV modules with glass front surfaces and 0.983 for the a-Si/a-Si/a-Si:Ge PV module with a Tefzel™ front surface. The index of refraction for glass is 1.526, versus 1.398 for Tefzel™.

Equation 9 provides a daily efficiency, η_{TA}, with both temperature and AOI corrections.

$$\eta_{TA} = \eta_T \cdot F_{AOIrc} / F_{AOI} \quad (9)$$

Spectral Correction

Daily efficiencies are corrected for spectral variation using the daily spectral mismatch correction M_d from Eqn. 3.

Equation 10 provides a daily efficiency, η_{TAM}, with temperature, AOI, and spectral mismatch corrections.

$$\eta_{TAM} = \eta_{TA} / M_d \quad (10)$$

An alternative for applying spectral corrections is the Sandia method [8], which uses an empirically based correction factor based on air mass, with polynomial coefficients that are determined using one or more days of outdoor performance measurements. This approach was included to show benefits and limitations of the two approaches. Daily efficiencies corrected for temperature, AOI, and spectral variation using the Sandia air-mass correction factor are identified as η_{TAS}.

Results and Summary

Table 4 lists the daily efficiencies, with and without corrections for temperature, AOI, and spectral variations. Daily efficiencies are normalized by the uncorrected average efficiency calculated for all days in September with clear days. This more readily shows relative differences and improvements of corrective methods. A smaller standard deviation indicates that a method provides a more consistent result and better accounts for daily and seasonal variations. Figures 1 through 4 provide graphic representations of the results in Table 4.

The daily efficiencies that were corrected for temperature, AOI, and spectral mismatch (η_{TAM}) yielded the smallest standard deviation, from 0.004 to 0.010. The use of the air-mass correction (η_{TAS}) increased the standard deviation for the CdTe and a-Si/a-Si/a-Si:Ge PV modules. In fact, the results were worse than when no corrections were applied (η). This result is supported by the modeling sensitivity analysis, where the CdTe and a-Si/a-Si/a-Si:Ge spectral mismatches were shown to be sensitive to water vapor amounts, which the air-mass correction does not address.

The CIGS PV module showed the least sensitivity to spectral variations. The standard deviation for the method correcting for only temperature and AOI was low, and the additional benefit of correcting for spectral mismatch was small. This is consistent with the expectation that technologies responsive to solar radiation over a greater range of wavelengths are less sensitive to variations in the solar spectrum.

Although the corrective methods in this work were applied to daily efficiencies of PV modules, they may also be applicable to the performance ratio for PV systems, a similar and dimensionless metric; consequently, this could result in improved methods for acceptance testing and verifying the performance of PV systems.

Table 4. Daily Efficiencies Corrected for Temperature, AOI, and Spectrum; and Normalized by the September Uncorrected Efficiency

Date	Single-crystal Si 0442				a-Si/a-Si/a-Si:Ge 1736				CdTe 5669				CIGS 5165			
	η_T	η_{TA}	η_{TAM}	η_{TAS}	η_T	η_{TA}	η_{TAM}	η_{TAS}	η_T	η_{TA}	η_{TAM}	η_{TAS}	η_T	η_{TA}	η_{TAM}	η_{TAS}
6/15/10	0.979	0.988	1.023	1.003	0.974	0.982	0.964	0.965	0.990	0.999	1.001	1.018	0.981	0.991	1.012	1.009
6/17/10	0.977	0.986	1.023	1.001	0.968	0.977	0.968	0.96	0.980	0.989	0.998	1.008	0.980	0.989	1.014	1.009
6/28/10	0.986	0.994	1.024	1.009	0.997	1.006	0.972	0.989	1.005	1.013	1.001	1.033	0.985	0.993	1.012	1.012
6/30/10	0.982	0.990	1.022	1.005	0.992	1.000	0.972	0.984	1.001	1.009	1.002	1.029	0.980	0.988	1.007	1.006
7/05/10	0.980	0.987	1.015	1.002	0.992	0.999	0.956	0.982	0.993	1.000	0.981	1.020	0.981	0.988	1.004	1.006
9/03/10	0.992	0.994	1.015	1.002	0.998	1.000	0.973	0.994	0.998	1.000	1.007	1.010	0.992	0.994	1.008	1.004
9/06/10	0.987	0.989	1.018	0.997	0.988	0.99	0.995	0.985	0.986	0.988	1.022	0.998	0.983	0.985	1.008	0.995
9/11/10	0.984	0.986	1.010	0.993	0.980	0.982	0.974	0.98	0.981	0.983	1.004	0.991	0.985	0.987	1.004	0.995
9/17/10	1.004	1.003	1.018	1.009	1.000	0.999	0.971	1.000	1.011	1.010	1.014	1.017	1.006	1.005	1.014	1.012
9/19/10	0.993	0.993	1.011	0.998	0.980	0.980	0.962	0.982	0.986	0.986	0.997	0.992	0.995	0.995	1.007	1.001
9/25/10	1.009	1.008	1.020	1.011	1.014	1.013	0.986	1.020	1.010	1.009	1.010	1.013	1.005	1.004	1.011	1.008
9/26/10	1.005	1.004	1.017	1.007	1.009	1.009	0.986	1.017	1.004	1.003	1.007	1.007	1.007	1.006	1.014	1.010
9/28/10	1.004	1.003	1.016	1.006	1.003	1.002	0.982	1.011	1.003	1.002	1.008	1.005	1.005	1.004	1.012	1.007
9/29/10	1.010	1.007	1.015	1.010	1.014	1.011	0.980	1.020	1.012	1.009	1.005	1.012	1.013	1.010	1.015	1.013
9/30/10	1.014	1.010	1.019	1.012	1.016	1.013	0.986	1.023	1.012	1.009	1.008	1.012	1.011	1.008	1.013	1.011
1/07/11	1.040	1.031	1.022	1.015	0.933	0.925	0.983	1.001	0.994	0.985	1.009	0.966	1.016	1.007	1.003	0.987
1/21/11	1.023	1.015	1.016	1.002	0.903	0.896	0.964	0.957	0.946	0.938	0.980	0.923	0.999	0.990	0.994	0.974
Average	0.998	0.999	1.018	1.005	0.986	0.987	0.975	0.992	0.995	0.996	1.003	1.003	0.996	0.997	1.009	1.003
Std. Dev.	0.017	0.012	0.004	0.006	0.029	0.030	0.010	0.021	0.016	0.017	0.010	0.025	0.013	0.008	0.005	0.010

REFERENCES

[1] C. Osterwald. Translation of Device Performance Measurements to Reference Conditions, *Solar Cells* 1986; **18**: 269–279.

[2] C. Gueymard. *User's Manual—SMARTS Code, Version 2.9.5 for Windows*. USA: Solar Consulting Services, 2005.

[3] C. Gueymard. "Updated Transmittance Functions for Use in Fast Spectral Direct Beam Irradiance Models." Proceedings of the 1994 Annual Conference, American Solar Energy Society, June 27–30, 1994, San Jose, California, pp. 355–360.

[4] D. Myers, K. Emery, C. Gueymard. "Terrestrial Solar Spectral Modeling Tools and Applications for Photovoltaic Devices." Proceedings of the 29th IEEE PV Specialists Conference, May 20–24, 2002, New Orleans, Louisiana.

[5] American Society for Testing and Materials, ASTM G 173-03. *Standard Tables for Reference Solar Spectral Irradiances: Direct Normal and Hemispherical for a 37° Tilted Surface*, West Conshohocken, PA: American Society for Testing and Materials, 2003.

[6] "Boulder Aeronet Data," http://aeronet.gsfc.nasa.gov/, last accessed 1/18/2012.

[7] "NASA Ozone Data," http://jwocky.gsfc.nasa.gov/teacher/ozone_overhead.html, last accessed 1/18/2012.

[8] D. King, W. Boyson, J. Kratochvil. Photovoltaic Array Performance Model, SAND2004-3535, Albuquerque, NM: Sandia National Laboratories, 2004.

[9] E. A. Sjerps-Koomen, E. A. Alsema, W. C. Turkenburg. A simple model for PV module reflection losses under field conditions, *Solar Energy*, 1997; **57**, 421–432.

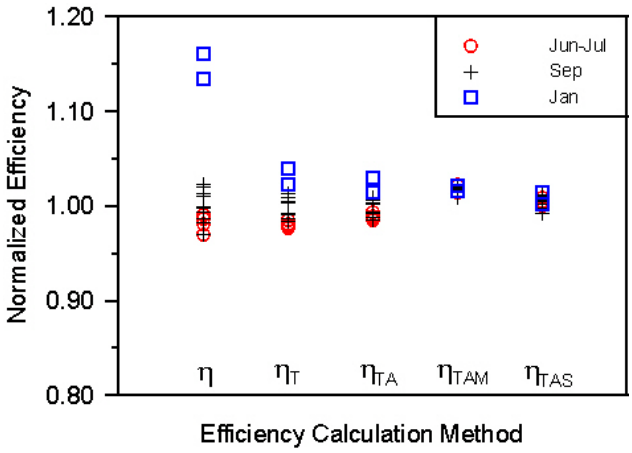

Figure 1 Normalized daily efficiencies for the single-crystal Si 0442 PV module: no corrections (η); temperature corrections (η_T); temperature and AOI corrections (η_{TA}); temperature, AOI, and spectral mismatch corrections, (η_{TAM}); and temperature, AOI, and Sandia air-mass corrections, (η_{TAS}).

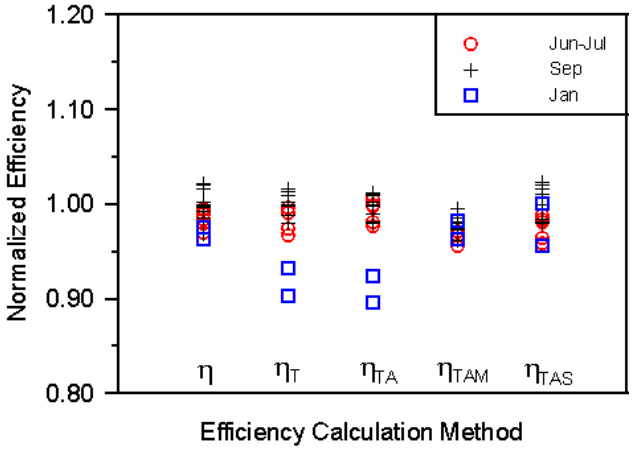

Figure 2 Normalized daily efficiencies for the a-Si/a-Si/a-Si:Ge 1736 PV module: no corrections (η); temperature corrections (η_T); temperature and AOI corrections (η_{TA}); temperature, AOI, and spectral mismatch corrections, (η_{TAM}); and temperature, AOI, and Sandia air-mass corrections, (η_{TAS}).

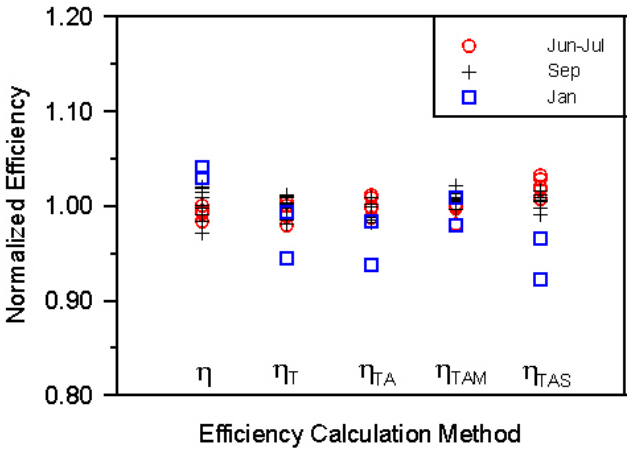

Figure 3 Normalized daily efficiencies for the CdTe 5669 PV module: no corrections (η); temperature corrections (η_T); temperature and AOI corrections (η_{TA}); temperature, AOI, and spectral mismatch corrections, (η_{TAM}); and temperature, AOI, and Sandia air-mass corrections, (η_{TAS}).

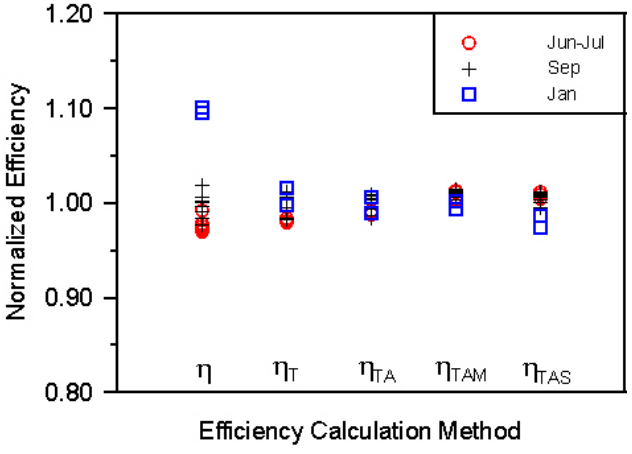

Figure 4 Normalized daily efficiencies for the CIGS 5165 PV module: no corrections (η); temperature corrections (η_T); temperature and AOI corrections (η_{TA}); temperature, AOI, and spectral mismatch corrections, (η_{TAM}); and temperature, AOI, and Sandia air-mass corrections, (η_{TAS}).